Tumour induced osteopenia due to phosphaturic mesenchymal sinonasal tumour presenting with delayed onset insufficiency fractures

Freda Jawan[1*], Weiling Lim[2], Joe Francis[1]

1. Department of Diagnostic Radiology, Changi General Hospital, Singapore

2. Department of Respiratory and Critical Care Medicine, Changi General Hospital, Singapore

* **Correspondence:** Freda Jawan, Changi General Hospital, 2 Simei St 3, 529889, Singapore (*freda.jawan@mohh.com.sg*)

Radiology Case. 2023 Jul; 17(7):8-16 :: DOI: 10.3941/jrcr.v17i7.4912

ABSTRACT

We present a case of a 48-year-old female who presented with epistaxis. Magnetic resonance imaging (MRI) revealed a mass within the left nasal cavity which was revealed to be a phosphaturic mesenchymal sinonasal tumour. The patient defaulted treatment at this stage and later re-presented with pelvic and groin pain for which plain radiographs and computed tomography (CT) scan demonstrated diffuse osteopenia and multiple pelvic fractures of varying ages. MRI of the pelvis and both thighs revealed abnormal marrow signal of the bones and confirmed the presence of pelvic fractures. Multiple pseudo-fractures were seen at both femurs and scapula. The radiological findings along with abnormal biochemical markers were attributed to the paraneoplastic entity of tumour induced osteomalacia, in the context of unresected phosphaturic mesenchymal tumour. The tumour was resected, and patient showed complete reversal of the associated biochemical abnormalities. This case exemplifies that with early identification and complete resection of the causative tumour, the prognosis is excellent.

Journal of Radiology Case Reports

www.RadiologyCases.com

CASE REPORT

CASE REPORT

A 48-year-old female without significant past medical history presented to our hospital's emergency department with sudden onset epistaxis. Initial nasal endoscopy revealed a mass in the left sphenoethmoid recess,v which was biopsied. MRI of the paranasal sinuses (Figure 1) confirmed the presence of a mass centered at the left posterior ethmoid sinus extending into the left nasal cavity and left sphenoid sinus. The mass demonstrated heterogeneous signal with hyperintense components on T1 weighted images and hyperintense signal intensity on T2 weighted images. There was avid enhancement of the mass post contrast administration. No intracranial extension or bony destruction was seen. Histologic evaluation of the mass revealed respiratory type mucosa covered tissue showing a non-circumscribed spindle cell proliferation in the subepithelial stroma with a hemangiopericytoma-like appearance, composed of bland spindle to stellate cells

associated with ectatic staghorn vessels. Overall features were suggestive of phosphaturic mesenchymal tumour. The patient was offered resection of the mass, but defaulted on appointments.

The patient re-presented to the emergency department two years later, with acute on chronic bilateral groin and lower limb pain. The pain was present for the past two years and has been getting worse over the recent 6 months which also made her wheelchair-bound. There was no history of trauma. The initial pelvis radiographs (Figure 2) showed fractures involving bilateral superior and inferior pubic rami.

Bilateral scapula radiographs performed (Figure 3) showed bilateral scapula fractures along their lateral cortices.

MRI of pelvis and bilateral thighs (Figure 4) confirmed the presence of multiple fractures involving bilateral pubic rami, sacrum and iliac bones. There were also multiple fracture lines/pseudo fractures at the medial aspect of both femoral necks and shafts. MRI also revealed abnormal high T2 signal intensity within the pelvic bones and both femurs, sparing the distal parts of both femurs.

In addition, CT scan of the abdomen and pelvis (Figure 5) performed for investigation of abdominal discomfort demonstrated generalized diffuse osteopenia along with bilateral rib, pelvic and sacral ala fractures of varying chronicity, some with callus formation.

In the context of unresected phosphaturic mesenchymal tumour and the presence of multiple atraumatic fractures, the patient was suspected to be having tumour induced osteomalacia (oncogenic osteomalacia) resulting in multiple insufficiency fractures. This was confirmed with biochemical markers which demonstrated low serum phosphate levels of 0.41 mmol/L [normal range: 0.65-1.65 mmol/L], low vitamin D levels at 7.1 Ug/L [normal range: 30-100 Ug/L], with evidence of increased phosphaturia where the 24 hour urine phosphate level was shown to be 35.88 mmol/day [normal range: 8.1-22.6 mmol/day]. Total corrected serum calcium was documented at 2.08 mmol/L [normal range: 2.1-2.6 mmol/L] and there was mildly elevated intact parathyroid levels at 8.01 pmol/L [normal range: 1.3-7.6 pmol/L]. In addition, alkaline phosphatase (ALP) levels were raised at 539 U/L [normal range: 32-193 U/L]. Serum anti-fibroblast growth factor 23 (FGF23) was high at 196 [normal range: $\leq$ 59].

The patient underwent internal fixation of both femurs in view of pain and inability to weight bear. The patient also underwent resection of the left ethmoidal-sphenoethmoidal phosphaturic mesenchymal tumour and subsequent biochemical investigations after 6 month duration showed near complete resolution of the abovementioned biochemical abnormalities. In particular, there was normalization of the serum anti-FGF23 at less than 14. In addition, reduction in levels of alkaline phosphatase at 193 U/L, normalization of vitamin D and serum phosphate levels at 30.6 Ug/L and 1.15 mmol/L, respectively, were also observed.

DISCUSSION

Epidemiology & Demographics:

Tumour induced osteomalacia (TIO), also known as oncogenic osteomalacia is a paraneoplastic syndrome associated with a co-existing underlying tumour. The underlying tumours associated with TIO are typically mesenchymal tumours of varying histological subtypes. The causative tumour, regardless of histology types are typically small, slow growing and in unusual anatomical location, which poses as a diagnostic challenge [1]. The most common histological type, accounting for 80% of cases, is phosphaturic mesenchymal tumour of the mixed connective tissue type. Other histologies include that of osteoblastoma-like tumours, ossifying fibrous-like tumours and non-ossifying fibrous-like tumours. While most of the causative tumour are benign, a few malignant variants have been described in literature [2,3].

Ectopic secretion of fibroblast growth factor 23 (FGF-23) results in several classical biochemical abnormalities which affects cartilage and bone mineralization, resulting in osteomalacia [4]. FGF-23 reduces renal reabsorption of phosphate which affects serum phosphate level [5]. In addition, FGF-23 induces reduction in serum 1,25(OH)2D (calcitriol) levels [6]. As a result, patients with TIO present with phosphaturia, low serum phosphate levels and inappropriately low serum calcitriol levels.

The epidemiology of TIO is relatively unknown given its rarity and has been shown to occur in a wide range of age groups with no specific gender predilection [7].

Clinical & Imaging findings:

Patients typically present with progressive bone pain and muscle weakness. Biochemically there is profound hypophosphatemia, phosphaturia and inappropriately low or normal calcitriol (1,25-dihydroxyvitamin D) which should typically be elevated in the presence of hypophosphatemia. Serum calcium and 25-hydroxyvitamin D are typically normal. In addition, serum alkaline phosphatase which is derived from bone, are typically elevated [8].

Radiological manifestations of TIO are that of osteomalacia which includes coarsened trabeculae, generalised osteopenia and presence of pseudo fractures called Looser's zones. Looser's zones occur from deposition of unmineralized osteoid at areas of stress or at nutrient vessels. On plain radiograph, Looser zones present as incomplete transverse lucent bands perpendicular to the cortex, classically occurring at medial femoral neck, pubic rami, and non-weight bearing aspect of bones such as lateral cortex of femoral shaft, lateral scapular border and iliac wings. Plain films are however unable to discriminate between the underlying aetiology of the osteomalacia and therefore requires correlation with clinical history and biochemical markers [9].

Thorough search for the causative tumour which may pose as a challenge given its unusual location and slow-growing nature [1]. Typical work up would include conventional cross sectional imaging utilizing CT or MRI. However, additional nuclear medicine studies such as Tc-99 sestamibi scan, octeotride scintigraphy and 18F-fluorodeoxyglucose (FDG)

Journal of Radiology Case Reports

www.RadiologyCases.com

Positron Emission Tomography (PET) may be helpful if CT or MRI fail to identify the lesion, as phosphoturic mesenchymal tumours have been shown to express somatostatin surface receptors, hence the abovementioned functional studies which utilize somatostatin analogs may be useful to localize the small but slow growing tumour[10].

Treatment & Prognosis:

Treatment for tumor-induced osteomalacia is resection of the underlying tumor. Successful and complete resection of the tumour results in normalization of the associated biochemical abnormalities within days to weeks. Healing of the bony abnormalities associated with osteomalacia typically occurs over a period of months [1].

Differential Diagnoses:

Differential diagnosis for tumour induced osteomalacia includes other disorders of impaired renal phosphorous reabsorption. Within the hereditary causes of phosphaturia are autosomal dominant hypophosphatemic rickets, X linked hypophosphatemia, hereditary hypophosphatemic rickets with hypercalciuria. Lastly, under the umbrella of hereditary and acquired causes, Fanconi's Syndrome should be considered.

Autosomal dominant hypophosphatemic rickets (ADHR)

ADHR occurs due to missense variant in gene encoding fibroblast growth factor 23 (FGF23). This prevents its cleavage thereby increasing circulating FGF23 levels [11]. These patients will present with positive family history, short stature, with variable presentation from childhood to adulthood [12]. Biochemically, it is indistinguishable from tumour induced osteomalacia, where serum FGF23 and parathyroid hormone levels will be raised, while serum calcitriol and calcium will be reduced. Radiographically, in addition to radiographic features of osteomalacia with pseudofractures, there are sclerotic bone lesions and generalised arterial calcifications present [13].

X linked hypophosphatemia (XLH)

XLH is the most common cause of hereditary hypophosphatemic osteomalacia [14]. The causative mechanism is due to defective phosphate regulating protein (PHEX) on the X-chromosome, resulting in renal tubular dysfunction [15]. Patients present with positive family history, short stature and typically present in childhood. Similar to ADHR, these patients are biochemically indistinguishable from tumour induced osteomalacia. Radiographically, similar to ADHR, there are sclerosing bone disease and features of osteomalacia [13]. In addition, peri-articular ossification around the acetabulae, proximal femora at tendon, ligament and capsule attachment is seen [16].

Hereditary hypophosphatemic rickets with hypercalciuria

Hereditary hypophosphatemic rickets with hypercalciuria occurs due to defective type 2c sodium-phosphate cotransporter [17]. Typical presentation occurs in childhood, between 6 months to 7 years of age [18]. It is biochemically distinct from tumour induced osteomalacia, XLH and ADHR, in that this group of patients would present with elevated calcitriol and hypercalciuria [19]. Radiologically, it presents with osteopenia and pseudofractures.

Fanconi's Syndrome

Fanconi's syndrome occurs due to a defect in the proximal renal tubule [20], secondary to either acquired (i.e., drug-induced causes, multiple myeloma) or hereditary forms (i.e., Glycogen storage disease type 1, Wilson's disease, cystinosis) [21]. Clinical presentation occurs in childhood and adulthood [20]. Biochemically, it is indistinguishable from TIO, ADHR and XLH. Radiographic features are as well nonspecific with pseudofractures, although a constellation of clinical features would suggest this differential diagnosis.

TEACHING POINT

The diagnosis of tumour induced osteopenia should be considered in patients who present with features of osteomalacia and biochemical features of phosphaturia without positive family history. Early identification of the underlying causative lesion typically results in good prognosis with complete reversal of the biochemical and radiological abnormalities.

REFERENCES

1. Drezner MK. Tumor-induced osteomalacia. Rev Endocr Metab Disord. 2001;2(2):175-86. PMID: 11705323.

2. Weidner N, Santa CD. Phosphaturic mesenchymal tumors. Cancer. 1987;59(8):1442-54. PMID: 3545439.

3. Folpe AL, Fanburg-Smith JC, Billings SD, et al. Most osteomalacia-associated mesenchymal tumors are a single histopathological entity: an analysis of 32 cases and a comprehensive review of the literature. Am J Surg Pathol. 2004;28(1):1-30. PMID: 14707860.

4. Larsson T, Zahradnik R, Lavigne J, et al. Immunohistochemical detection of FGF-23 protein in tumors that cause oncogenic osteomalacia. Eur J Endocrinol. 2003;148(2):269-76. PMID: 12590648.

5. Kaul M, Silverberg M, Dicarlo EF, et al. Tumor-induced osteomalacia. Clin Rheumatol. 2007;26(9):1575-1579. PMID: 17225058.

6. Shimada T, Hasegawa H, Yamazaki Y, Muto T, Hino R, Takeuchi Y, Fujita T, Nakahara K, Fukumoto S, Yamashita T. FGF-23 is a potent regulator of vitamin D metabolism and phosphate homeostasis. J Bone Miner Res. 2004;19(3):429-435. PMID: 15040831.

7. Dadoniene J, Miglinas M, Miltiniene D, Vajauskas D, Seinin D, Butenas P, Kacergius T. Tumour-induced osteomalacia: a literature review and a case report. World J Surg Oncol. 2016;14(1)4. PMID: 26744291.

Journal of Radiology Case Reports

www.RadiologyCases.com

8. Jan de Beur SM. Tumor-induced osteomalacia. JAMA. 2005;294(10):1260-7. PMID: 16160135.

9. Pitt MJ. Rickets and osteomalacia. In: Resnick D, ed. Diagnosis of bone and joint disorders. 4th ed. Philadelphia, Pa: Saunders, 2002;1901-1946. ISBN: 0721689213.

10. Sahoo J, Balachandran K, Kamalanathan S, Das AK, Patro DK, Halanaik D, Badhe B. Tumour(s) induced osteomalacia- a curious case of double trouble. J Clin Endocrinol Metab. 2014;99(2):395-98. PMID: 24297794.

11. Benet-Pagès A, Lorenz-Depiereux B, Zischka H, White KE, Econs MJ, Strom TM. FGF23 is processed by proprotein convertases but not by PHEX. Bone. 2004;35(2):455-62. PMID: 15268897.

12. Ruppe M, Jan de Beur S. Disorders of phosphate homeostasis. In: Rosen CJ, ed. Primer on the metabolic bone diseases and disorders of mineral metabolism . 7th ed . Washington, DC: American Society for Bone and Mineral Research, 2008;317-25. ISBN: 978-1-118-45388-9.

13. Laurent MR, De Schepper J, Trouet D, Godefroid N, Boros E, Heinrichs C, Bravenboer B, Velkeniers B, Lammens J, Harvengt P, Cavalier E, Kaux J-F, Lombet J, De Waele K, Verroken C, van Hoeck K, Mortier GR, Levtchenko E and Vande Walle J. Consensus recommendations for the diagnosis and management of x-linked hypophosphatemia in Belgium. Front Endocrinol (Lausanne). 2021;12:641543. PMID: 33815294.

14. Alizadeh Naderi AS, Reilly RF. Hereditary disorders of renal phosphate wasting. Nat Rev Nephrol. 2010;6(11):657-65. PMID: 20924400.

15. Francis F, Hennig S, Korn B, et al. A gene (PEX) with homologies to endopeptidases is mutated in patients with X-linked hypophosphatemic rickets. Nat Genet. 1995;11(2):130-6. PMID: 7550339.

16. Polisson RP, Martinez S, Khoury M, Harrell RM, Lyles KW, Friedman N, Harrelson JM, Reisner E, Drezner MK. Calcification of entheses associated with X-linked hypophosphatemic osteomalacia. N Engl J Med. 1985;313(1):1-6. PMID: 4000222.

17. Bergwitz C, Roslin NM, Tieder M, Loredo-Osti JC, Bastepe M, Abu-Zahra H, Frappier D, Burkett K, Carpenter TO, Anderson D, Garabedian M, Sermet I, Fujiwara TM, Morgan K, Tenenhouse HS, Juppner H. SLC34A3 mutations in patients with hereditary hypophosphatemic rickets with hypercalciuria predict a key role for the sodium-phosphate cotransporter NaPi-IIc in maintaining phosphate homeostasis. Am J Hum Genet. 2006;78(2):179-92. PMID: 16358214.

18. Drezner M. Phosphorus homeostasis and related disorders. In: Bilezikian J, Raisz L, Rodan G, eds. Principles of bone biology. 2nd ed. San Diego, Calif: Academic Press, 2002; 330. ISBN: 9780123738844.

19. Tieder M, Modai D, Samuel R, Arie R, Halabe A, Bab I, Gabizon D, Liberman UA. Hereditary hypophosphatemic rickets with hypercalciuria. N Engl J Med. 1985;312(10):611-7. PMID: 2983203.

20. Van't Hoff W. Fanconi syndrome. In: Davidson A, Cameron J, Grunfeld J, et al, eds. Oxford textbook of clinical nephrology. 3rd ed. New York, NY: Oxford University Press, 2005; 962-71. ISBN: 978-0198508243.

21. Earle KE, Seneviratne T, Shaker J, Shoback D. Fanconi's syndrome in HIV+ adults: report of three cases and literature review. J Bone Miner Res. 2004;19(5):714-21. PMID: 15068493.

Journal of Radiology Case Reports

www.RadiologyCases.com

FIGURES

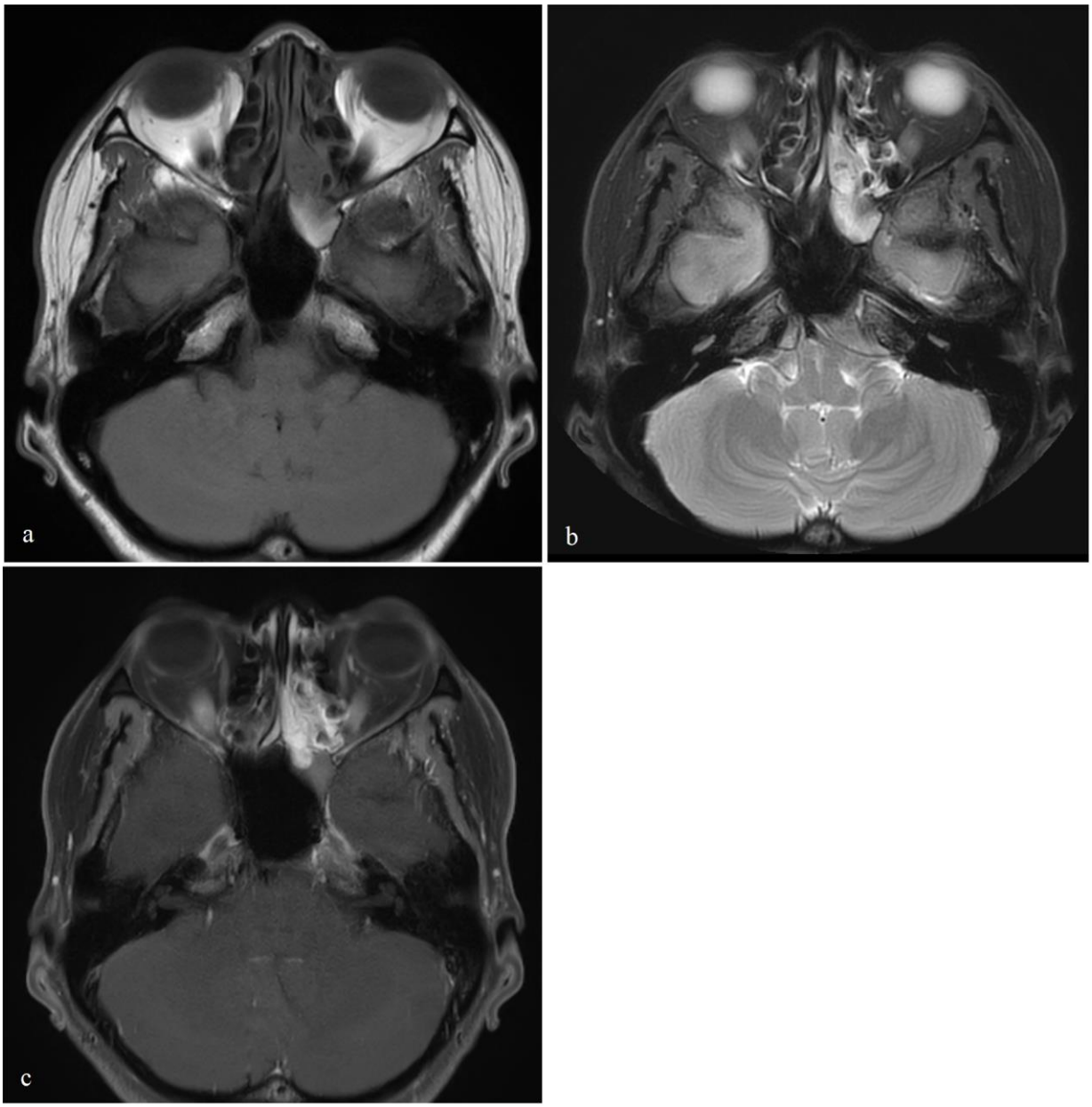

Figure 1: 48-year old female presented to emergency department with sudden onset epistaxis of 1 day duration.

Findings:
(a) Axial T1-weighted MRI image of the paranasal sinus shows mass centered at the left posterior ethmoid sinus extending into the left nasal cavity and left sphenoid sinus. The mass demonstrated heterogeneous signal intensity with hyperintense component.
(b) Axial T2-weighted MRI image of the paranasal sinus showed hyperintense signal intensity.
(c) Axial post contrast T1-weighted MRI image of the paranasal sinus, after administration of 10 ml of Clariscan, demonstrated areas of avid contrast enhancement of the mass lesion.

Technique (a): Axial T1-weighted MRI of the paranasal sinuses in a 3T Philips Ingenia. TR=574.22, TE=9.00, Flip Angle=100.00 and slice thickness=4.00 mm.
Technique (b): Axial T2-weighted MRI of the paranasal sinuses in a 3T Philips Ingenia. TR=3005.62, TE=80.00, Flip Angle=90.00 and slice thickness=4.00 mm.
Technique (c): Axial T1-weighted MRI of the paranasal sinuses post administration of intravenous contrast media - Clariscan (10 ml) in a 3T Philips Ingenia. TR=512.21, TE=9.00, Flip Angle=100.00 and slice thickness=4.00 mm.

Journal of Radiology Case Reports
www.RadiologyCases.com

Figure 2 (right): 48-year-old female with bilateral groin and thigh pain.

Findings: Frontal view radiograph of the pelvis shows displaced fractures of bilateral superior pubic rami (arrows), and fractures of the inferior pubic rami (arrowhead).

Technique: Frontal posteroanterior view radiograph of the pelvis with settings at a kVp of 81 and mAs of 25.

Journal of Radiology Case Reports

www.RadiologyCases.com

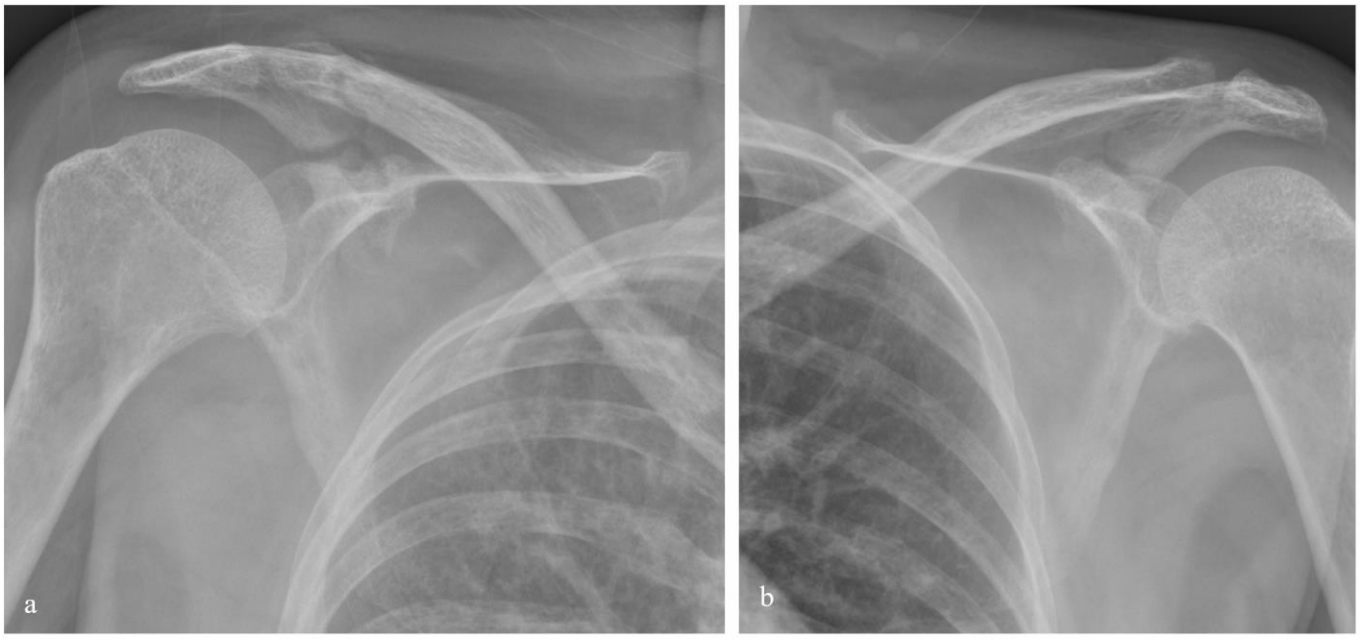

Figure 3: 48-year old female with bilateral scapula pain.

Findings:
(a) Frontal projection of the right shoulder radiograph demonstrates pseudofracture involving the lateral border of the right scapula.
(b) Frontal projection of the left shoulder radiograph demonstrates pseudofracture involving the lateral cortex of the left scapula.

Technique: Frontal view radiograph of the scapula with settings at a kVp of 70 and mAs of 6.

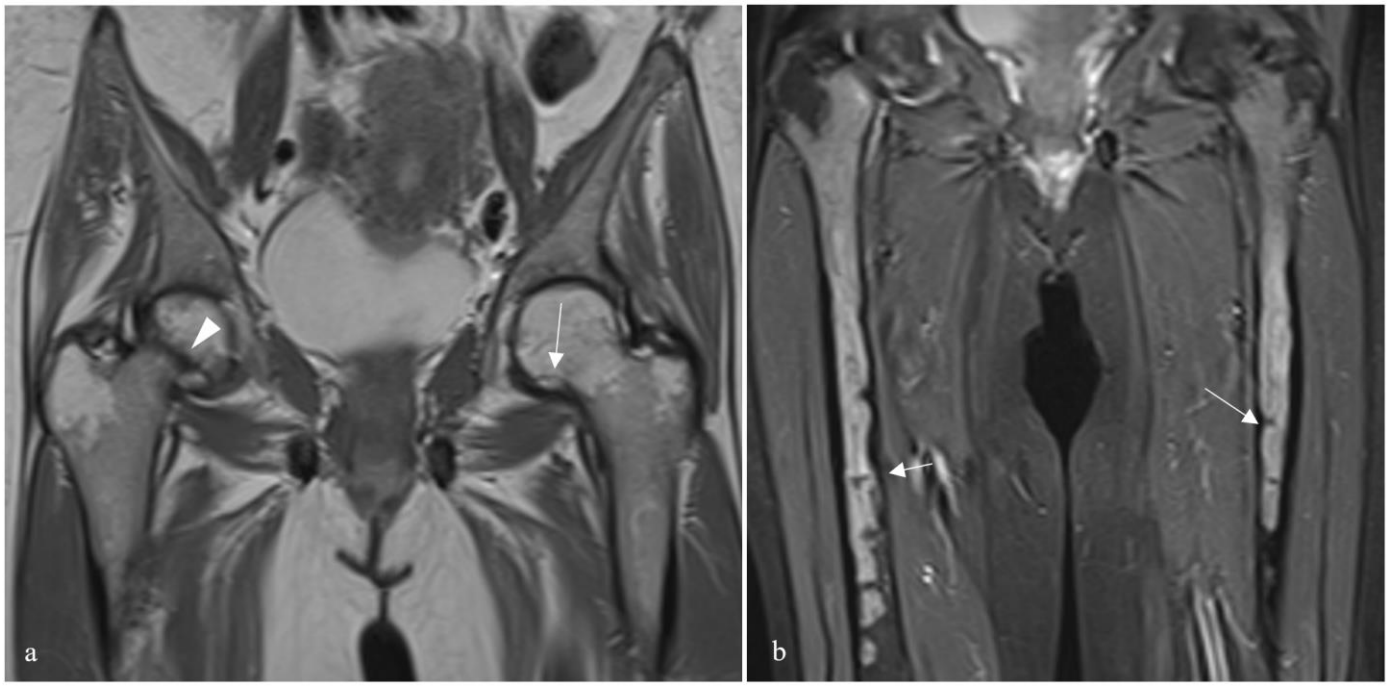

Figure 4: 48 years old female with bilateral groin and thigh pain.

Findings:
(a) Coronal proton density-weighted (PD) MRI image of the pelvis demonstrated an undisplaced fracture of the right femoral neck (arrowhead). Faint PD hypointense line at the medial cortex of the left femoral neck (arrow), suspicious for fracture.
(b) Coronal turbo inversion recovery magnitude (TIRM) demonstrated transverse hypointense lines at the femoral shafts bilaterally at its medial and lateral femoral cortices incompletely traversing the femoral shaft, suspicious for pseudofractures.

Technique:
(a) Coronal proton density-weighted (PD) MRI of the pelvis in a 1.5T Siemens Magnetom Sola scanner. TR=4430.00, TE=34.00, Flip angle = 143.00 and slice thickness 4.50 mm.
(b) Coronal turbo inversion recovery magnitude (TIRM) MRI of bilateral thigh in a 1.5T Siemens Magnetom Sola scanner. TR=3720.00, TE=33.00, TI=160.00, flip angle=150.00, slice thickness=4.00 mm.

Journal of Radiology Case Reports

www.RadiologyCases.com

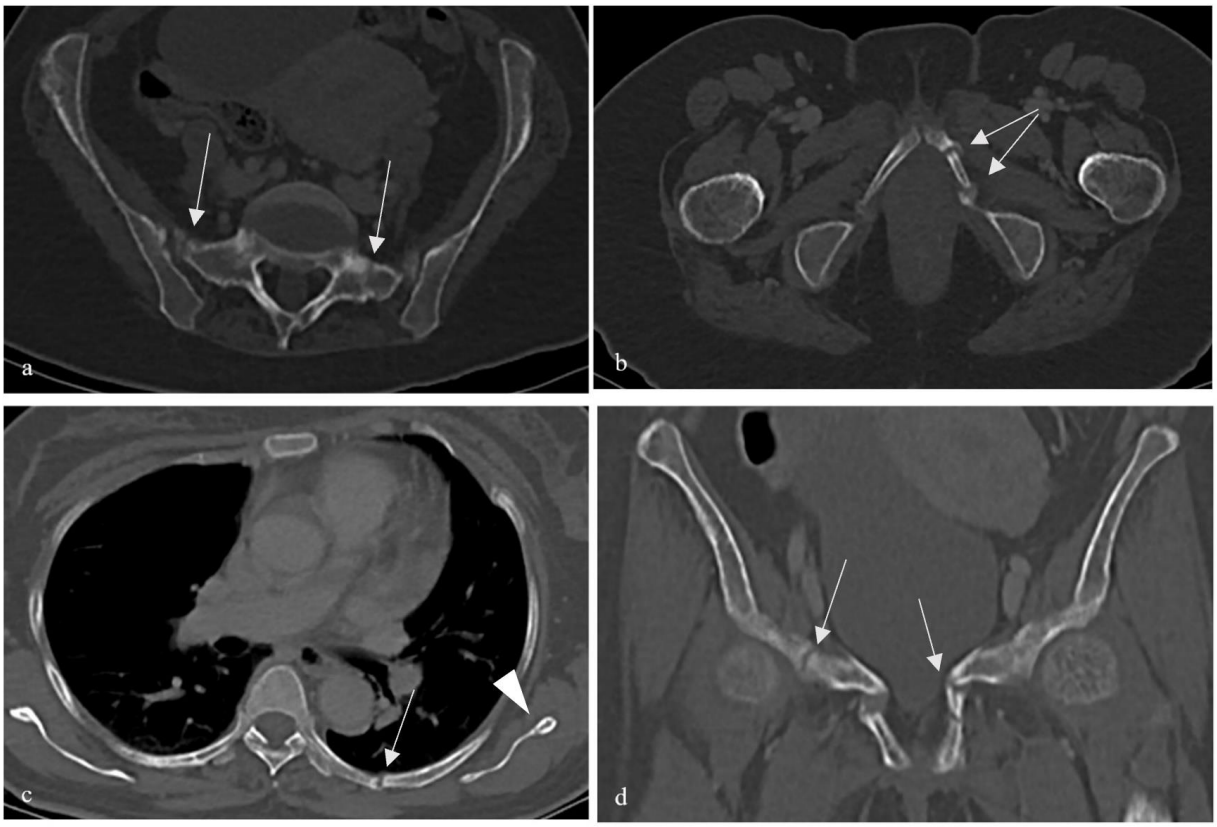

Figure 5: 48 years old female with bilateral groin and thigh pain.

Findings:
(a) Axial section of the pelvis demonstrates bilateral sacral fractures (arrows).
(b) Axial section of the pelvis demonstrates inferior pubic rami fractures (arrows).
(c) Axial section of the lower thorax demonstrates a few left side rib fractures (arrow), as well as fracture of the lateral scapula (arrowhead).
(d) Coronal section of the pelvis demonstrates multiple superior pubic rami fractures (arrows).

Technique: Axial CT abdomen pelvis in venous phase with coronal reconstruction in a TOSHIBA Aquilion ONE scanner. Slice thickness = 5mm. kVP 120, DLP 206.50 mGy.cm.

Journal of Radiology Case Reports

www.RadiologyCases.com

Etiology	Paraneoplastic syndrome due to underlying tumour, typically mesenchymal tumours.
Incidence	Rare disease, with approximately 1000 cases reported worldwide
Gender ratio	No known gender predilection
Age predilection	Wide age range, no age predilection
Risk factors	No known risk factors
Treatment	Identification of causative tumour and complete resection which will resolve the associated osteomalacia, pseudofractures and biochemical abnormalities
Prognosis	Good prognosis with complete resolution of associated features with complete tumour resection.
Findings on imaging	Plain radiograph: Looser zones, incomplete transverse lucent lines perpendicular to the cortex, occurring at medial femoral neck, pubic rami, and non-weight bearing aspect of bones such as lateral cortex of femoral shaft, lateral scapula border and iliac wings. MRI: Perpendicularly oriented T1w hypointense lines at the cortices of the bones with marrow oedema

Table 1: Summary table of oncogenic osteomalacia.

Diagnosis	Etiology, Mechanism	Imaging
Tumour induced osteomalacia (TIO)	• Paraneoplastic syndrome due to underlying tumour, typically mesenchymal tumour. • Negative family history • Variable age of presentation • Biochemically: ↑FGF23, ↓calcitriol, ↓calcium, ↑PTH	Xray: features of osteomalacia and pseudofractures
Autosomal dominant hypophosphatemic rickets (ADHR)	• Due to missense variant in gene encoding fibroblast growth factor 23 (FGF23), preventing its cleavage, thereby increasing circulating FGF23 levels [11] • Positive family history • Variable presentation of childhood to adulthood • Biochemically: ↑FGF23, ↓calcitriol, ↓calcium, ↑PTH [13]	X-ray: Sclerosing bone disease Pseudofractures Generalised arterial calcifications [13]
X-linked hypophosphatemia (XLH)	• Most common cause of hereditary hypophosphatemic osteomalacia • 1 in 20,000 live births [14] • Positive family history • Presents in childhood • Renal tubular dysfunction due to defective PHEX (phosphate-regulating protein with homology to endopeptidases on X chromosome) gene on Xp22.1 chromosome [15] • Biochemically: ↑FGF23, ↓calcitriol, ↓calcium, ↑PTH [13]	X-ray: Dense bones, pseudofractures and enthesopathy [13]
Hereditary hypophosphatemic rickets with hypercalciuria (HHRH)	• Defective type 2c sodium-phosphate cotransporter [17] • Onset in childhood • Positive family history • Presents in childhood • Biochemically: ↑FGF23, ↑calcitriol*, ↑calcium, ↓PTH [13], *Normal-elevated calcitriol (differentiates it from XLH and ADH) (Tieder et al.)	Xray: Osteopenia, pseudofractures
Fanconi's syndrome	• Defective proximal renal tubule • Inherited forms i.e. glycogen storage disease type 1, cystinosis, Wilson's disease • Acquired forms: medications (i.e. Valproate, aminoglycosides), multiple myeloma [21] • Biochemically: ↑FGF23, ↓calcitriol, ↓calcium, ↑PTH, metabolic acidosis, aminoaciduria [13]	Pseudofractures together with other features of underlying disease

Table 2: Differential diagnosis table for hypophosphatemic osteomalacia.

Journal of Radiology Case Reports

www.RadiologyCases.com

ABBREVIATIONS

ADHR = Autosomal dominant hypophosphatemic rickets
FGF23 = Fibroblast growth factor 23
HHRH = Hereditary hyposphotemic rickets with hypercalciuria
PTH = parathyroid hormone
TIO = Tumour induced osteomalacia
XLH = X-linked hypophosphatemia

KEYWORDS

Phosphaturic mesenchymal tumour; Tumour induced osteopenia; Sinonasal tumour; Insufficiency fractures; Pseudofracture

Online access

This publication is online available at:
www.radiologycases.com/index.php/radiologycases/article/view/4912

Peer discussion

Discuss this manuscript in our protected discussion forum at:
www.radiolopolis.com/forums/JRCR

Interactivity

This publication is available as an interactive article with scroll, window/level, magnify and more features.
Available online at www.RadiologyCases.com

Published by EduRad

www.EduRad.org